Essential Readings in Light Metals: Aluminum Reduction Technology.
Edited by Geoff Bearne, Marc Dupuis and Gary Tarcy.

From *Light Metals 1981*, Gordon M. Bell, Editor

THE EFFECT OF SOME OPERATING VARIABLES ON FLOW IN ALUMINUM REDUCTION CELLS

E.D. Tarapore
Staff Research Engineer, Process Development
Reduction Research
Kaiser Aluminum & Chemical Corporation
Permanente, California

The significant effects of current distribution and magnetic field on reduction cell operation have been recognized for many years. The current distribution and magnetic field are determined partly by the design of the cell and partly by operating variables such as anode current distribution, condition of the cathode bottom, and the influence of adjacent cells. Recent work has been done on design considerations for stable cell operation but very little on cell operation under conditions removed from ideal.

A model to calculate fluid flow in aluminum reduction cells has been used to determine the effects of cell design and operating variables for a prototype 185 kA cell. The effects of non-ideal magnetic fields or current distribution, caused for example by complex steel effects, anode change or mis-set anodes, have been calculated. The calculations are compared with flows measured in the prototype cell.

INTRODUCTION

The trend in modern aluminum reduction technology is towards cells rated at increasingly higher amperage. As cell amperage rating increases, so does the importance of the associated electromagnetic effects. These effects are increasingly taken into consideration in the design of aluminum reduction cells.

For reasons of computational practicality, though, the effects of many smaller details of the design cannot be taken into consideration. Furthermore, cells do not operate under ideal conditions. Operating variables such as anode current distribution, the condition of the cathode bottom, and the condition of adjacent cells influence cell operation. This work uses a method developed earlier [1] to determine the effects of cell design and operating variables for a prototype 185 kA cell.

Anode changes and muck formation alter the smooth operation of the cell by changing the current distribution in the metal pad. Large local horizontal currents are generated. These currents were calculated using an analytical model to obtain a local voltage distribution in the metal pad. The effect of these currents on fluid flow has been determined.

The calculations are compared with flows measured in the prototype cell for verification of the model.

THE MODEL

The basic model used to calculate fluid flow in a reduction cell has been described in detail in an earlier paper [1]. A brief description is included here to complement the discussion of the present model. All vector fields and variables were referenced to the coordinate system shown in Figure 1 located at the center of the steel shell.

The potential distribution in the cell cavity was calculated using a finite element method to solve the conduction equation in two dimensions. Current and current density within the cell were calculated from the potential distribution using Ohm's law. Current flow in the X-direction

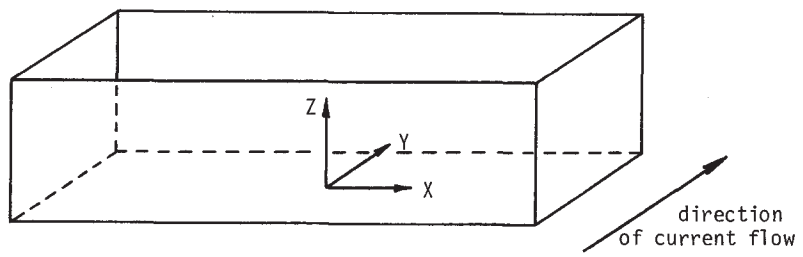

Figure 1. Coordinate System for 185 kA Cell

was calculated from the current distribution measured in the collector bars of the prototype cell. A similar method was used to calculate the overall Y-direction current in the metal pad that results from the slight imbalance between the upstream and downstream collector bar currents caused by the slight difference in resistance between the two runs of bus.

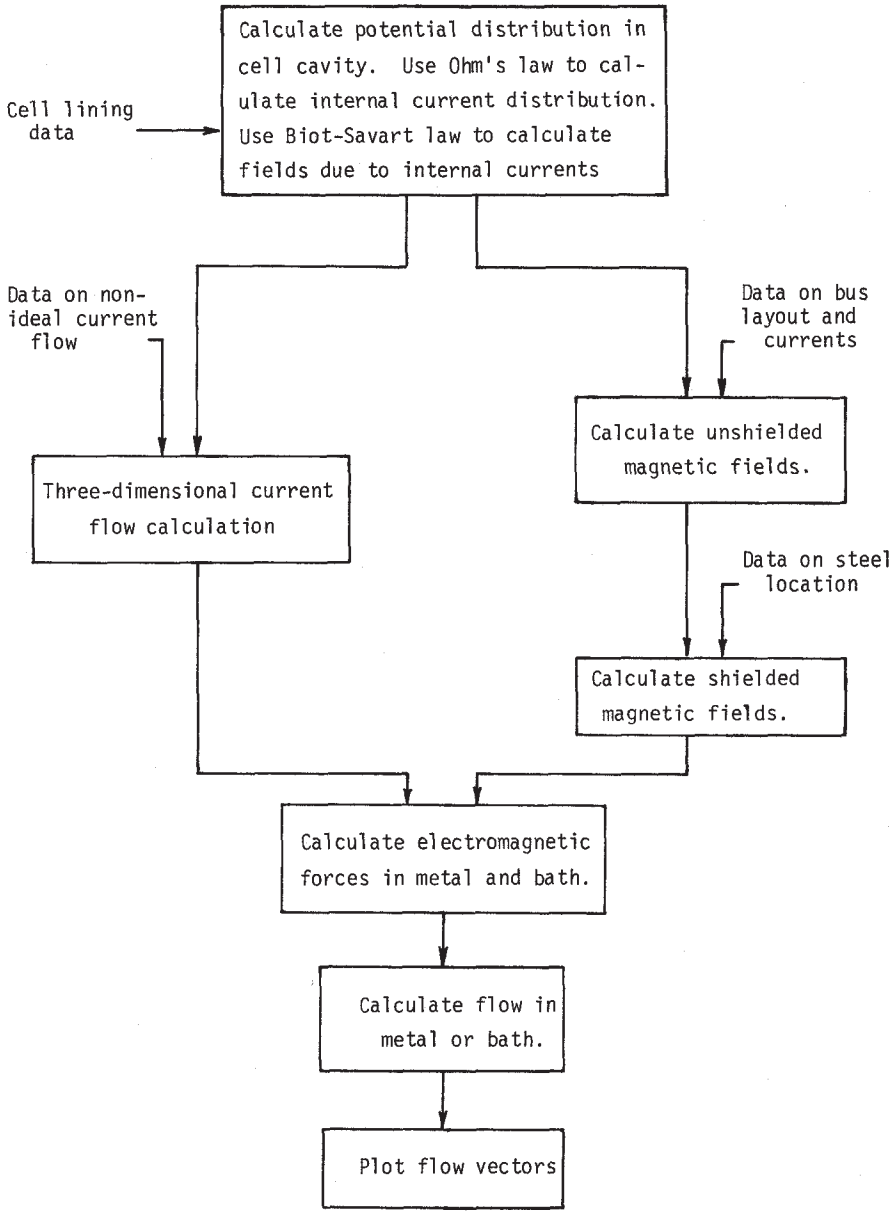

Figure 2. Block Diagram Outlining Calculation

Magnetic fields in the cell were calculated from the internal currents and currents in the bus bars around the cell using the Biot-Savart law. The steel shell and superstructure significantly alter the magnetic field and act to shield the metal pad and bath from the influence of the external conductors. The shielding effect was calculated using a magnetic dipole model [2] of the steel shell (not including the superstructure). This technique was found to have better accuracy than the use of a simple magnetic attenuation factor [3].

The electromagnetic forces in the metal and bath were calculated next and used to calculate metal and bath flow. The turbulent Navier-Stokes equations were solved with the aid of a finite difference computer program [4] which solves for the turbulent viscosity within the melt using a two-equation (k-ε) model of turbulence. The overall calculation is presented in the form of a block diagram in Figure 2.

The chain of calculations described above and in Figure 2 has several checkpoints where results of each phase of the calculation may be reviewed. At these points, data may also be introduced to simulate conditions other than ideal. This technique was used to determine the effect of operating variables.

During anode change, for example, Figure 3(a) shows a schematic presentation of the current flow in the metal pad below the disconnected anode. As the bath is of comparatively high resistance, current flow in the bath is predominantly vertical, and virtually all horizontal current flow occurs in the metal pad. The situation in the metal pad was modeled as shown in Figure 3(b). The insulated vertical boundaries essentially confine the region of horizontal current flow. The lower horizontal boundary represents the carbon cathode surface with uniformly redistributed current. The insulated part of the upper horizontal boundary represents the disconnected anode(s) with a uniform vertical current flow across the rest of this boundary. For a single center anode being changed, therefore, the insulated region represents half the anode width. The conducting region represents the immediately adjacent live anode. For an end anode that has been disconnected, the insulated region represents the two adjacent live anodes. The two-dimensional Laplace equation was solved with the given boundary conditions to yield the horizontal currents in the metal pad:

$$\frac{J_H}{J} = \sum_{n=1}^{\infty} \frac{2 \operatorname{Sin} \frac{n\pi}{3}}{n\pi \operatorname{Sh} \frac{n\pi}{L} H} \operatorname{Sin} \frac{n\pi}{L} x \operatorname{Ch} \frac{n\pi}{L} z$$

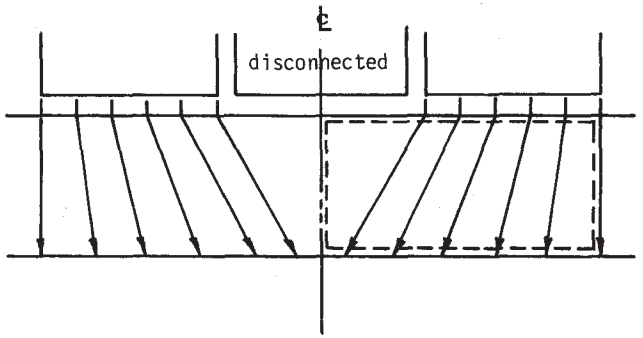

Figure 3(a). Schematic Representation of Current Flow Below a Disconnected Anode. Dotted lines outline area shown below.

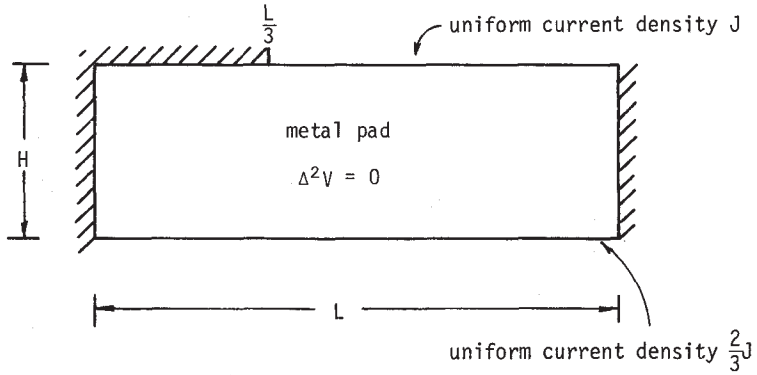

Figure 3(b). Boundary Conditions

represents an insulated boundary.

The magnitude of the horizontal current is greatest near the boundary between the insulated and the live anode. The horizontal currents were averaged in the metal pad immediately below the discontinuity and plotted as a function of the uniform vertical anode current density J in Figure 4. The effect of changing a corner anode is more than double the effect of changing one of the other anodes in terms of the generation of horizontal currents in the metal pad. These values were used in the calculation of the effect of an anode change on metal circulation. Similar techniques were used to calculate redistribution of current in the metal pad brought about by the presence of an insulating layer of muck on the cathode bottom.

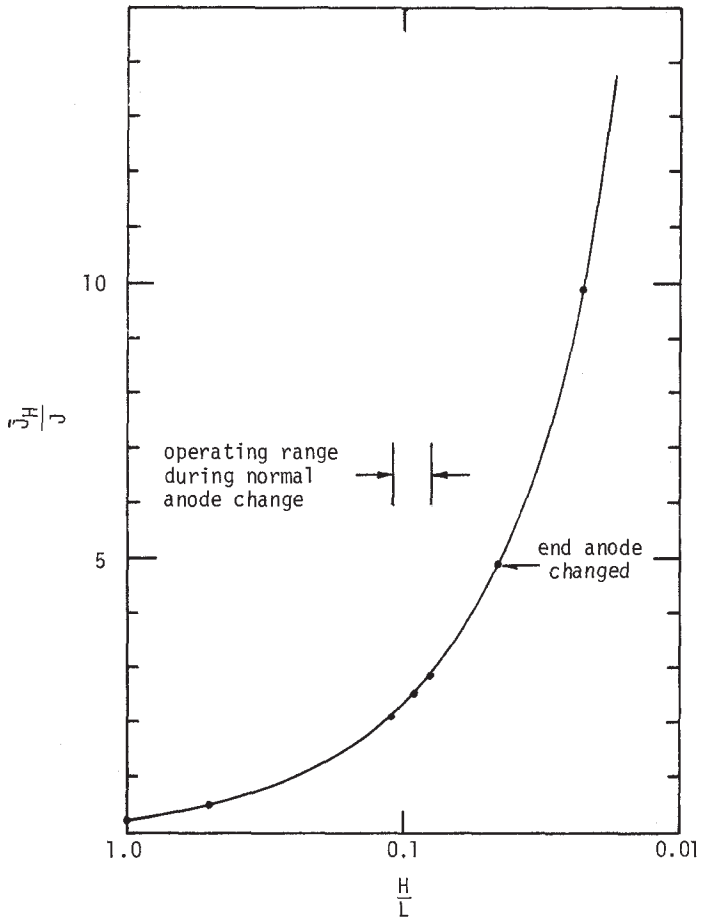

Figure 4. Horizontal Currents Generated During Anode Change

RESULTS AND DISCUSSION

The calculated and measured magnetic fields are shown in Figures 5 and 6, respectively. The calculated field was symmetrical and underestimated the measured field by ∿13%. The asymmetry in the measured field was small, but it produced a complete change in the flow pattern of the metal. The flow pattern calculated from the calculated field was symmetrical and is shown in Figure 7(a). Flow occurred in four large vortices with two smaller vortices on the upstream side. Maximum velocities are about 12 cm/sec. The flow pattern calculated from the measured field is shown in Figure 7(b). The flow pattern was asymmetrical with one large vortex in the cell and two counter vortices in two opposite corners.

The metal flow was measured in the cell using a rod dissolution technique [5] simultaneously with the magnetic field. The measured flow is shown in Figure 8. The metal flow calculated using the measured magnetic field approximates the measured flow well in every area except on the tap end upstream side. The points of flow reversal were predicted exactly by the calculation. This clearly shows the effect of changes in magnetic field on the flow in the metal pad. It also indicates that greater accuracy is necessary in the calculation of the steel effect for the overall magnetic field to be adequately characterized.

The direction of flow on the tap end upstream side was opposite to the calculated flow direction. This condition was thought to be related to the presence of muck under the anodes on the side of the cell. The redistribution of current due to the presence of muck was calculated as indicated earlier and superposed on the idealized current distribution calculated earlier. The calculated metal flow pattern is shown in Figure 9. The vortex at the tap end of the cell grew at the expense of the large asymmetrical vortex. This reversed the flow direction and brought the entire calculated velocity profile in line with the measured data.

It should be noted that relatively small inaccuracies in the characterization of the electric currents and magnetic field were responsible for significant changes in calculated flow in the metal pad. This underscores the need for equal attention to be paid to all areas of the calculation outlined in Figure 2. Sophisticated methods of calculation in one area without comparable accuracy in all other areas yield diminished returns.

Horizontal currents generated by anode change also alter the metal pad velocities and the topography of the bath/metal interface until the new anode picks up on load. The effect of a disconnected anode was a flow diversion outward to the sidewall in this area, Figure 10. The effect of the disconnection in overall flow can vary from large [Figure 10(a)] to small [Figure 10(b)], depending on the location of the anode vis-a-vis the undisturbed flow pattern. If the anode was in a region where flow was directed to the wall, this effect would be greatly enhanced. Otherwise, the overall flow would not be much affected.

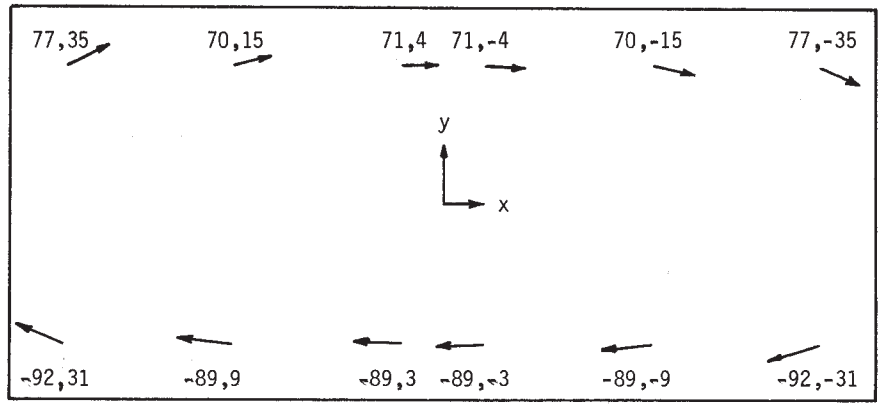

(a) Horizontal B_x, B_y

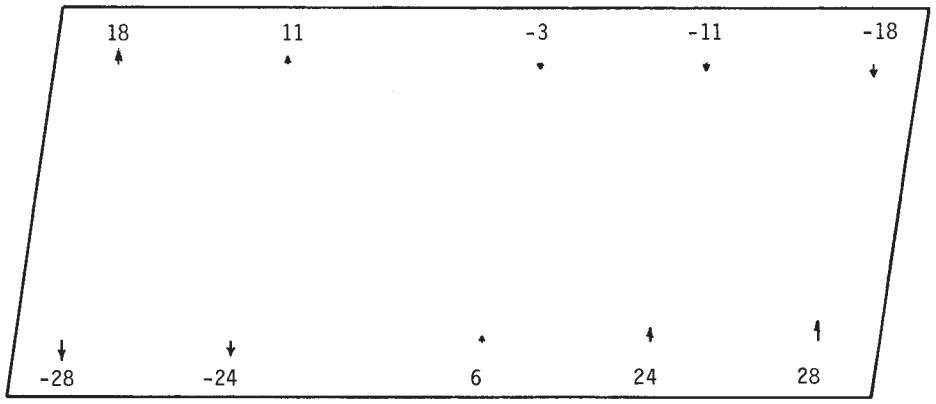

(b) Vertical B_z

Figure 5. Magnetic Field Calculated in 185 kA Prototype Cell

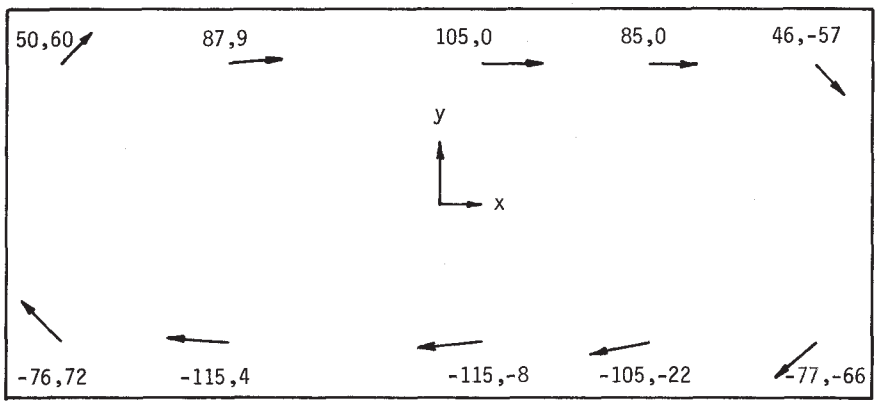

(a) Horizontal B_x, B_y

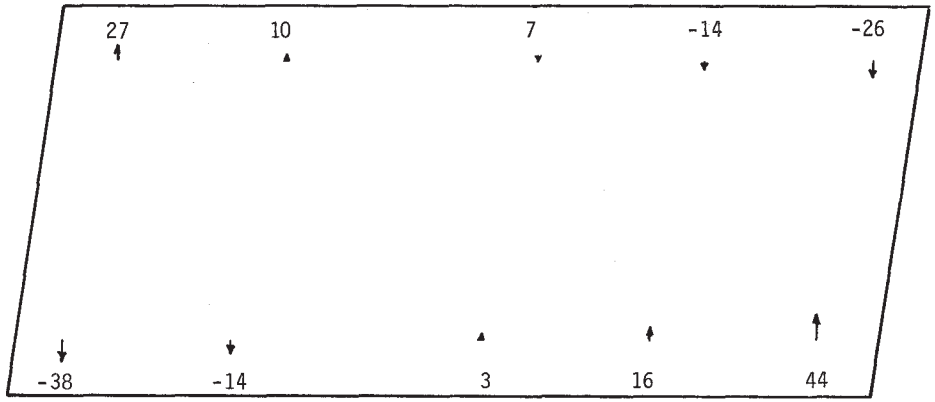

(b) Vertical B_z

Figure 6. Magnetic Field Measured in Prototype Cell at 183.1 kA

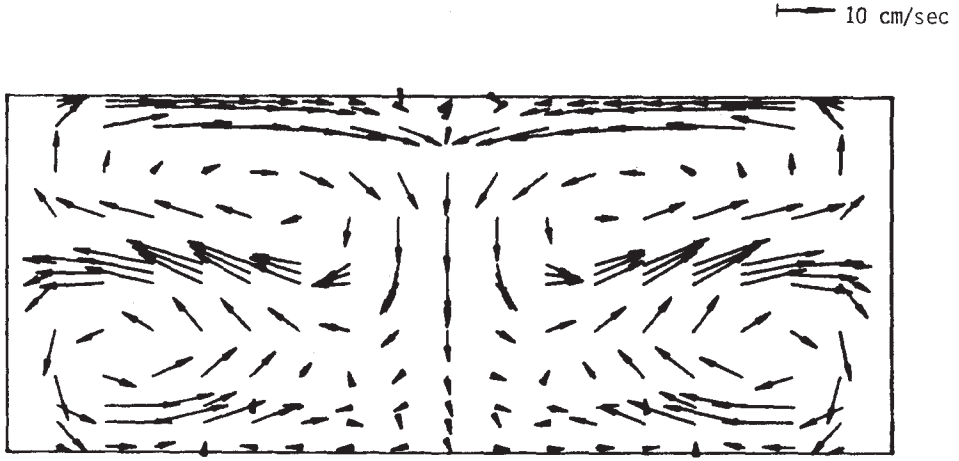

Figure 7(a). Metal Flow Calculated with Calculated Magnetic Field

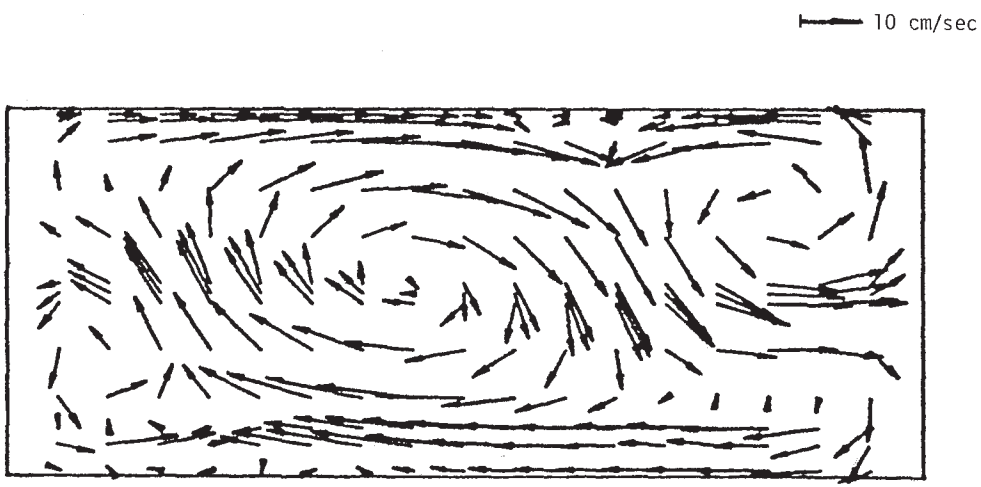

Figure 7(b). Metal Flow Calculated with Measured Magnetic Field

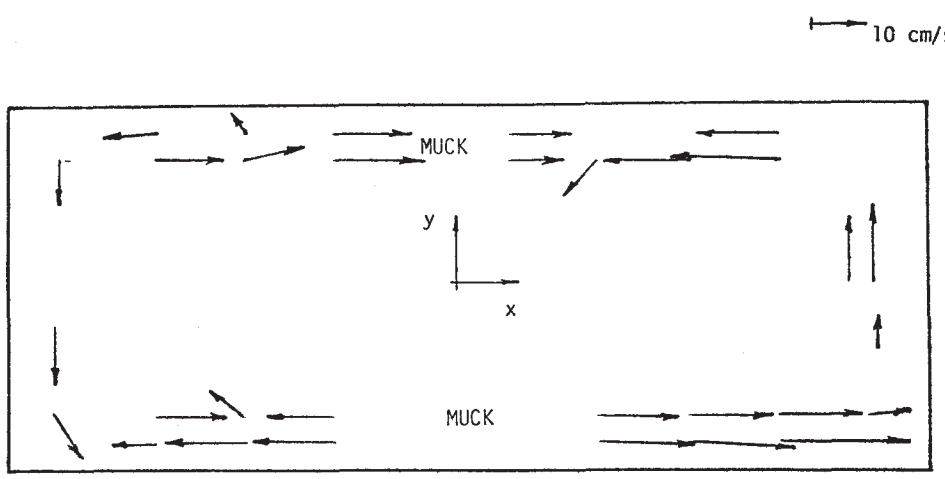

Figure 8. Measured Velocities in the Metal Pad

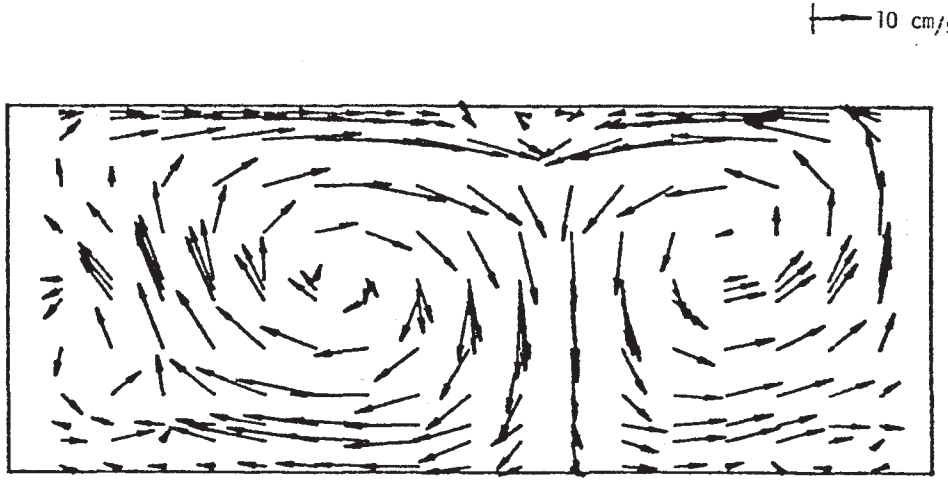

Figure 9. Metal Flow Recalculated with Horizontal Current Distribution Calculated Assuming Muck on Bottom of Cell Cavity

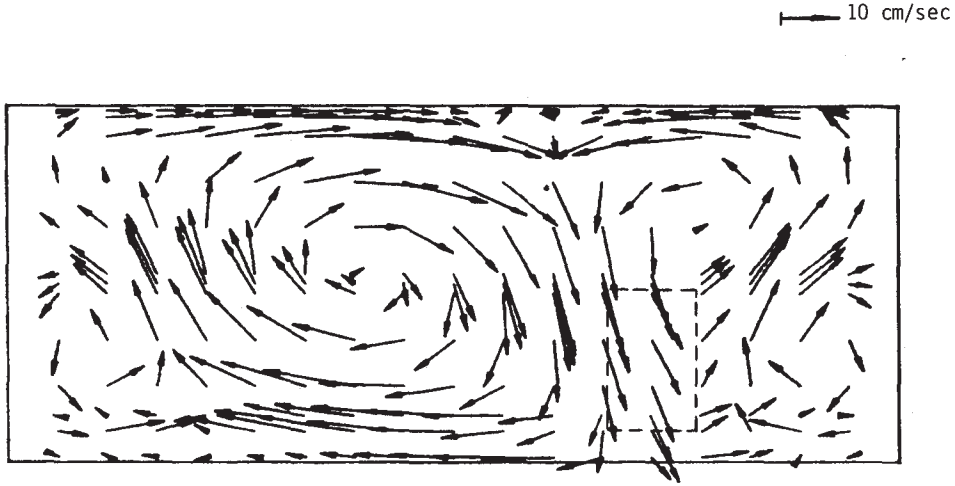

Figure 10(a). Metal Flow Calculated Assuming the Removal of Anode Number 3

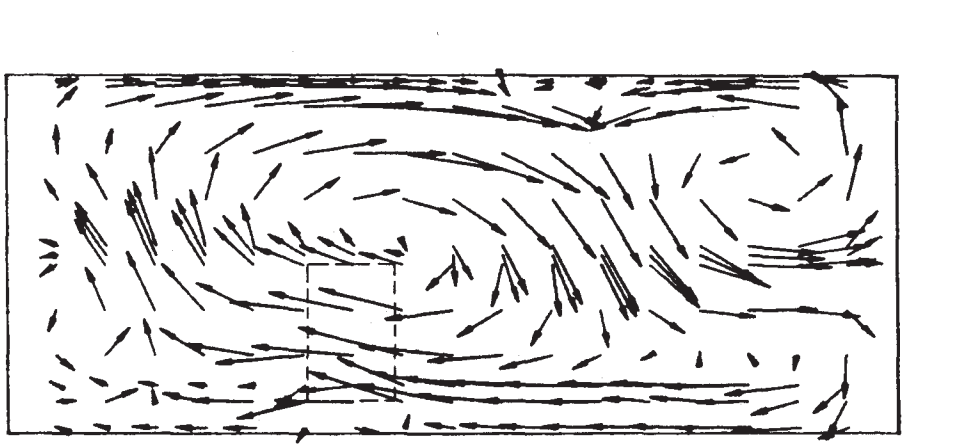

Figure 10(b). Metal Flow Calculated Assuming the Removal of Anode Number 6

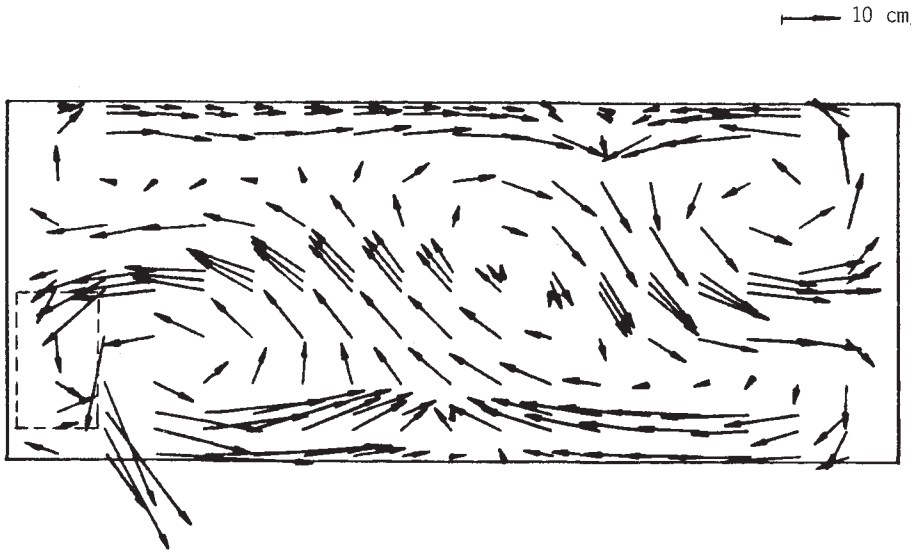

Figure 11. Metal Flow Calculated Assuming the Removal of Anode Number 9

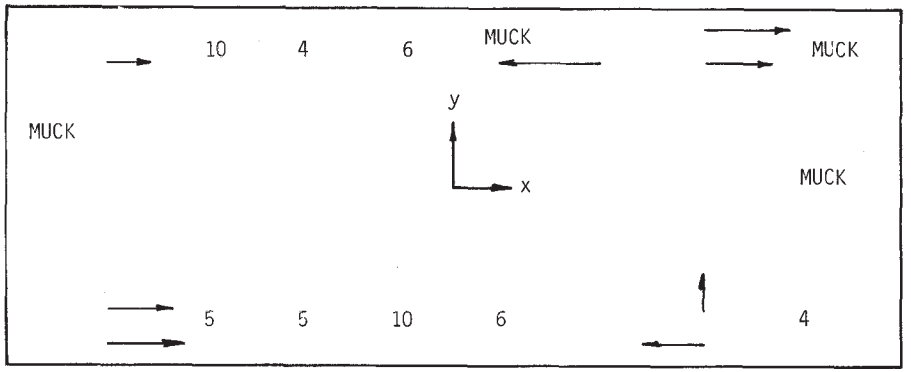

Figure 12. Measured Velocities in the Metal with Anodes 9 and 10 Disconnected

The effect of changing corner anodes was shown to be greater in Figure 4. The flow pattern obtained when one corner anode was disconnected is shown in Figure 11. Disconnecting both anodes at one end of the cell significantly changes the current flow and magnetic field. The resultant metal flow is shown in Figure 13. The flow measured under these circumstances is shown in Figure 12. There is good agreement in the region of the two disconnected anodes. The deleterious effects of horizontal currents generated when both end anodes are disconnected could be avoided by also altering the cathode current distribution if the disconnection were expected to last for a considerable length of time.

CONCLUSIONS

A model for the calculation of fluid flow in aluminum reduction cells has been used to calculate the effect of some operating variables on current distribution and hence on metal flow. The results were in generally good agreement with measurements made under exactly conforming conditions.

ACKNOWLEDGEMENT

I wish to thank Roger Johnson for the experimental data used in the verification of the model.

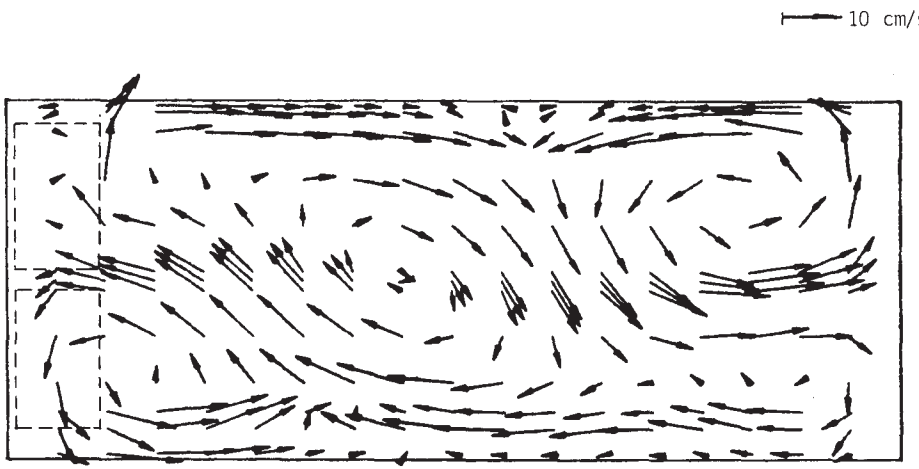

Figure 13. Metal Flow Calculated Assuming the Removal of Anodes 9 and 10

REFERENCES

1. E.D. Tarapore, "Magnetic Fields in Aluminum Reduction Cells and Their Influence on Metal Pad Circulation," Light Metals 1979, vol. 1, pp 541-550.

2. Th. Sele, "Computer Model for Magnetic Fields in Electrolytic Cells Including the Effect of Steel Parts," Met. Trans., vol. 5B, (1974), pp 2145-2150.

3. R.F. Robl, "Influence by Steel Shell on Magnetic Fields within Hall-Heroult Cells," Light Metals 1978, vol. 1, pp 1-13.

4. D. Sharma, "Details of an Efficient Computational Procedure for the Prediction of Convective Heat, Mass and Momentum Transfers," Report ATG/TN/DN/41, Advanced Technology Group, Dames and Moore, Denver, Colorado.

5. A.R. Johnson, "Metal Pad Velocity Measurements in Aluminum Reduction Cells," Light Metals 1978, vol. 1, pp 45-48.